Fast Algorithms for the Simulation of Electromagnetic Metal Forming*

M. Stiemer[1], J. Unger[2], H. Blum[1], B. Svendsen[2]

[1]Chair of Scientific Computing, TU Dortmund
[2]Chair of Mechanics, TU Dortmund

Abstract

Despite the comprehensive understanding of the modeling and numerical simulation of electromagnetic metal forming that has recently been gained, the simulation of real forming situations is still a challenging task due to the large computational resources required. A bottleneck is the computation of the electromagnetic fields, since 100.000 up to several million unknowns are required to represent the geometry of a typical forming device. The purpose of this article is to present new techniques to speed up the simulation of electromagnetic metal forming with particular emphasis on the computation of the electromagnetic fields. An acceleration of the electromagnetic field computation is a significant step towards a virtual design of electromagnetic forming processes.

Keywords:

Modeling, Electromagnetic Metal Forming

1 Introduction

The description of many phenomena in nature as well as of many engineering processes is based on multiphysical models. Consider, e.g., electromagnetic metal forming (EMF), a high speed forming process in which strain rates of over 10^3 s^{-1} arise. It is driven by he Lorentz force, a material body force, that results from the interaction of a pulsed magnetic field with eddy currents induced by the magnetic field. The magnetic field is triggered by a tool coil adjacent to the work piece which is excited by the discharging current of a capacitor bank. Although EMF offers certain advantages over other forming methods such as, e.g., an increased formability, a reduce in wrinkling, reduced tool making costs, the opportunity to

This work was carried out in the context of the German National Science Foundation (Deutsche Forschungsgemeinschaft (DFG)) Research Group FOR 443. The authors wish to thank the DFG for its financial support.

combine forming and assembly operations or the avoidance of contact, its industrial use has been limited to joining tubular semifinished materials up to know. The reason for this is the highly dynamic nature of this process inhibiting its monitoring and control. This emphasizes the significance of reliable simulations of this process to identify relevant process parameters and to optimize them.

During the last years, great progress in the simulation of coupled electromagnetic mechanical processes has been achieved. In case of electromagnetic forming, e.g., a fully coupled three dimensional simulation environment has been developed [1, 2]. It is based on the formulation of an appropriate continuum mechanical thermodynamic consistent model for electrically conducting viscoplastic solids under the influence of magnetic fields [3, 4] accounting for the rate dependency of the material typical for those strain rates arising in electromagnetic forming. Further, an algorithmic formulation for the computation of three dimensional time varying transient magnetic fields in the presence of inhomogeneous moving materials has been developed [e.g. 5, 6, 6]. Of particular importance was the implementation of a reliable coupling scheme between the electromagnetic field computation and the mechanical simulation [see 5, 6, 6]. Further, methods to correctly consider dynamical contact between the work piece and a forming tool had to be developed. A significant gain in efficiency could finally be reached by use of efficient solid shell finite elements [e.g. 7, 8] which combine the great efficiency a two dimensionally based model offers with the convenience of nodal degrees of freedom.

Although the physics behind the coupled process and its numerical requirements have been completely understood, the simulation of real forming situations represents still a scientific challenge. The reason for this is the large number of unknowns necessary to model the geometry of a real forming device sufficiently accurate. In this respect, electromagnetic forming perfectly mirrors the situation in computational electromagnetics and particularly in the numerical computation of interactions between electromagnetic fields and mechanical structures. While the scientific foundations are well understood, efficiency is a major issue of present research.

The purpose of this article is to present new approaches to increasing the computational efficiency of the simulation of electromagnetic metal forming processes. Particularly, methods to speed up the electromagnetic field computation are discussed. The paper is organized as follows. In Section 2, the mechanical model is briefly summed up and some remarks concerning its fast and accurate numerical simulation are given. Then, an efficient model for the electromagnetic subsystem is introduced (Section 3). Strategies for coupling the electromagnetic and the mechanical subsystems are then presented in Section 4. Section 5 is concerned with adaptive techniques to speed up the electromagnetic field computation. The paper ends with a discussion of applications and further perspectives (Section 6).

2 Accelerating the Mechanical Simulation

We first give a brief review of the mechanical model. Starting point for the relevant electromagnetic thermoelastic multifield model [3, 4] is the weak momentum balance

$$\int_{B_\mathrm{r}} (\varrho_\mathrm{r} \ddot{\boldsymbol{\xi}} - \boldsymbol{f}) \cdot \boldsymbol{\xi}_* + \boldsymbol{P} \cdot \nabla_\mathrm{r} \boldsymbol{\xi}_* = \int_{\partial B_\mathrm{r}} |\mathrm{cof}(\boldsymbol{F}) \boldsymbol{n}_\mathrm{r}| \, \boldsymbol{t}_\mathrm{c} \cdot \boldsymbol{\xi}_* \tag{1}$$

with respect to the referential configuration $B_\mathrm{r} \subset R$ of the work piece for all corresponding test fields $\boldsymbol{\xi}_*$ vanishing on those parts of the current boundary ∂B_c where $\boldsymbol{\xi}$ is specified. Here, $\boldsymbol{\xi}$ represents the deformation field, $\boldsymbol{f} = \det(\boldsymbol{F})\, \boldsymbol{j} \times \boldsymbol{b}$ the Lorentz force (density), $\boldsymbol{P}$ the first Piola-Kirchhoff stress, $\boldsymbol{F} := \nabla_\mathrm{r} \boldsymbol{\xi}$ the deformation gradient, and $\boldsymbol{t}_\mathrm{c}$ the current boundary traction. The mechanical model relations are completed by the specification of the material model. For a given thermodynamic state of the mechanical structure, $\boldsymbol{P}$ can, as usual, be computed from the free Helmholtz-energy stored in the material. The evolution of its density ψ_r is determined by the evolution of certain inner variables, which are, in this case, the accumulated inelastic strain, the elastic left Cauchy Green tensor and the temperature. Characteristic for the viscoplastic material model is an activation approach for modeling the evolution of the logarithmic inelastic strain. See [3, 4] for a detailed discussion.

The choice of adequate element formulations for the finite element discretization of the above mechanical model depends on geometrical properties of the structure under consideration. While continuum elements lead to satisfactory results for the simulation of tube compression, an efficient simulation of sheet metal forming requires more sophistication. Here, a solid shell formulation has been employed combining the convenience nodal degrees of freedom offer with the efficiency of a two dimensional formulation [e.g. 7, 8]. To avoid locking, modern element technology has been referred to.

3 Electromagnetic Field Computation in 3D

Electromagnetic phenomena are modeled by Maxwell's equations. This is a system of four partial differential equations for four fields, the magnetic field h, the magnetic flux density b, the electric field e and the electric displacement field d (see e.g. [9]). For the materials considered here, we have linear relations $h = \mu b$, where μ denotes the permeability of the vacuum, and $e = \epsilon_0 d$, where ϵ_0 denotes the permittivity of the vacuum. In many cases, Maxwell's equations possess wave solutions. In electromagnetic forming, however, the occurring wave lengths are much longer than the distances relevant for the forming process. Hence, the quasistatic approximation to Maxwell's equations applies (see [9, 10]), and high frequent displacement currents may be neglected. Principally, the field problem has to be solved in the whole space $\mathbb{R}^3$. However, due to the a priori known fast decay of electromagnetic dipole fields, the problem can be tackled in a large bounded open set $\Omega \subset \mathbb{R}^3$ with sufficient accuracy. In electrically conducting areas of Ω, e is related to an electric current j by a further constitutive material law. For the materials considered here, this relation simply reads $j = \gamma e$ with the electrical conductivity γ.

To compute the b and the e field, two new fields, a vector field $a = a(x, t)$ with curl $a = b$

and a scalar field $\phi = \phi(x,t)$ with

$$j = \gamma \left(-\frac{\partial a}{\partial t} - \nabla\phi - v \times \operatorname{curl} a \right) \tag{2}$$

are introduced to solve the field relations. Here, v denotes the velocity of a material point with respect to a fixed frame. The Lorentz force acting on an electrically conducting body, whose points are subject to a movement with velocity field v is given by

$$f_L = j \times b = -b \times \gamma e = \operatorname{curl} a \times \gamma \left(-\frac{\partial a}{\partial t} - \nabla\phi - v \times \operatorname{curl} a \right) . \tag{3}$$

In the case of an Eulerian formulation, the conductivity $\gamma = \gamma(x,t)$ depends on the spatial variable x and on the time t. We have $\gamma \neq 0$ if and only if the point x is covered by the work piece Σ at time t or is a point of the spatially fixed tool coil S. In the following discussion, we omit the electromotive forces $v \times \operatorname{curl} a$. From a practical point of view this is justified, since finite element simulation which consider these terms did hardly produce other results than finite element simulations omitting them (see [10]). Moreover, in the context of an arbitrary Lagrangian Eulerian reformulation of the electromagnetic subsystem, electromotive forces will implicitly be considered again. An Eulerian description of the evolution of the electromagnetic field is now given by

$$\operatorname{curl} \frac{1}{\mu} \operatorname{curl} a - \gamma \frac{\partial a}{\partial t} = \gamma \nabla\phi . \tag{4}$$

For discretization with finite elements, we consider – as usual – the week formulation, i.e., we search $a \in L^2(H_{\operatorname{curl},0}(\Omega))$ such that

$$\begin{aligned} \int_\Omega \frac{1}{\mu} \operatorname{curl} a \, \operatorname{curl} a^* + \int_\Omega \gamma \, a^* \, \frac{\partial a}{\partial t} &= -\int_S \gamma \, a^* \, \nabla\phi \\ \int_S \nabla\phi \, \nabla\phi^* &= 0 \end{aligned} \tag{5}$$

for all $a^* \in H_{\operatorname{curl},0}(\Omega)$ and for all $\phi^* \in H_0^1(\Sigma \cup S)$. Trial functions are taken from the spaces $L^2(H_{\operatorname{curl},0}(\Omega))$ of functions that map the time interval under consideration into the space $H_{\operatorname{curl},0}(\Omega)$ of spatially varying square integrable functions whose (weak) curl is still a square integrable function. On Ω, we can chose initial data $a(0) = 0$, boundary data $n \times a(x,t) = 0$, $x \in \partial\Omega$ and boundary data $\phi(x,t) = U(x,t)$, $x \in \partial\Omega \cap \partial S$.

Unfortunately, the system (5) does not provide a unique vector potential. Any temporally constant non zero field $\tilde{a}$ with $\operatorname{curl} \tilde{a} = 0$ fulfilling suitable boundary conditions may be added to a to obtain a solution different from a. Unique solvability can be granted by imposing an additional *gauge* of the vectorpotential, e.g., the Coulomb gauge, demanding $\operatorname{div} a = 0$ in Ω. The corresponding saddlepoint problem possesses a unique solution. This can e.g. be shown by proving that a suitable temporal semidiscretization leads to purely spatial problems that fulfill a Ladyshenskaya Babushka Brezzi (LBB) condition. However, saddlepoint problems of the size that is typical for practical forming problems, require large computational efforts, since both equations, equation (4) and the gauge condition need to be discretized using suitable discrete spaces. Particularly, the discrete LBB condition needs

to be fulfilled.

Hence we will now present another model for the electromagnetic subsystem: Starting point is the observation that equation (4) implies the relation

$$\text{div}\,\frac{\partial a}{\partial t} = -\Delta\phi \tag{6}$$

in electrically conducting areas. Equation (6) can now be used to introduce a Coulomb gauge implicitly in areas with a positive electrical conductivity $\gamma(x,t) > 0$. This is simply done by replacing (6) by

$$\Delta\phi = 0\,. \tag{7}$$

We solve equation (7) in areas with positive electrical conductivity first and take $\nabla\phi$ as input quantity in (4) afterwards. Then any vectorpotential fulfilling (4) is forced to have zero divergence in electrically conducting areas. The associated Lorentz forces can be computed via equation (3). The problem remains not gauged in all areas with $\gamma(x,t) = 0$. From a physical point of view, this is no problem, since any potential a fulfilling (4) in areas with $\gamma = 0$ possesses the same $b = \text{curl}\,a$, an this is the only quantity of physical significance there.

For given $\gamma \in L^2(L^2(\Omega))$ the semi-gauged electromagnetic field problem has a solution with a unique curl, and for two solutions a_1 and a_2 we always have $a_1(x,t) = a_2(x,t)$ where $\gamma(x,t) \neq 0$. The main idea of the proof of this statement is to impose an *artificial conductivity* in the air region and to control the amount of conductivity by a regularization parameter. The resulting *regularized* problems are purely parabolic and properly gauged. It can be shown that sequences of regularized problems can be chosen in such a way that they converge towards a field that represents a solution of equation 4. A detailed account of the techniques involved is given in [11] in a more abstract setting. Similar ideas have been applied by S. Zaglmayr in [12].

The lack of uniqueness in our model system (5) leads to severe numerical problems, since the linear systems of equations resulting from a finite element discretization will be singular. Hence, a straight forward application of numerical standard solvers will fail. Nevertheless, certain discretizations of the non gauged formulation can efficiently be solved [see 13]. The crucial idea is to perform an approximate Helmholtz decomposition on the discrete level and to treat the curl-free component in another way than the component with vanishing divergence. Such an algorithmic Helmholtz decomposition requires the choice of certain finite elements. From the work of R. Hiptmair, [e.g. 14], it is known that Nédélec elements [15, 16] allow for such a treatment, contrary to nodal elements.

Nédélec elements are the natural choice to discretize electromagnetic problems in three dimensions, both in the case of a saddle point formulation or in the case of an non gauged formulation. In the former case they provide a good approximation to the curl of the vector potential and simultaneously fulfill the discrete LBB-condition. In the lowest order version for hexahedral meshes, the test- and trial functions on an individual mesh element possess the form

$$b_k(x) = \begin{pmatrix} a_{11}^{(k)} + a_{12}^{(k)}x_2 + a_{13}^{(k)}x_3 + a_{14}^{(k)}x_2x_3 \\ a_{21}^{(k)}x_1 + a_{22}^{(k)} + a_{23}^{(k)}x_3 + a_{24}^{(k)}x_1x_3 \\ a_{31}^{(k)}x_1 + a_{32}^{(k)}x_2 + a_{33}^{(k)} + a_{34}^{(k)}x_1x_2 \end{pmatrix} \tag{8}$$

with $x = (x^{(1)}, x^{(2)}, x^{(3)})^\top$, $a_k, b_k \in \mathbb{R}$, $k = 1, 2, 3$. The degrees of freedom are integral means

$$M_i(b) = \int_{\Gamma_i} b \cdot t_i \tag{9}$$

over the edges Γ_i, $i = 1, \ldots, 4$ of the tetrahedron. This choice of degrees of freedom enforces only the continuity of tangential components of the resulting discretization over element faces, while normal components may jump. This corresponds to the smoothness properties of piecewise analytic functions that are globally in $H_{\mathrm{curl}}(\Omega)$, implying that Nédélec elements provide a conformal approximation. Nédélec elements for tetrahedra are constructed in a similar way.

Next, we discuss the temporal discretization, which is based on a discontinuous finite element method. These methods are on the one hand known to be particularly good suited for long-term computations and facilitate on the other hand error estimation for the fully discrete scheme, since they are Galerkin methods (e.g. [17, 18, 19, 20]).

Let $T_1 = t_0 < t_1 < \ldots < t_n = T_2$ be a partition of $I = [T_1, T_2]$ and $I_n = (t_{n-1}, t_n)$ the nth time interval with length $k_n = t_n - t_{n-1}$. Let $\mathcal{S}_n$ be the finite dimensional space used in the nth timestep for spatial discretization. Let further

$$V_q = \left\{ v \in L^2\left(H^1(\Omega) \,:\, v|_{I_n} \in V_{q,n}\right)\right\},$$

with $q \in \mathbb{N}_0$ and with

$$V_{q,n} = \left\{ v \,:\, v = \sum_{j=0}^{q} t^j \, u_j \,, u_j \in \mathcal{S}_n \right\},$$

be the time-space test- and trial space. For brevity, we will write

$$A(u, v) = \frac{1}{\mu} \int_\Omega \operatorname{curl} u \, \operatorname{curl} v \,.$$

An approximation $a^h \in V$ to the vector potential a is computed via the fully discrete scheme

$$\int_{I_n} A(a^h, v) + \int_{I_n} \left[\left(\frac{\partial a^h}{\partial t}, v \right)_{\Sigma \cup S} + \left([a^h]_{n-1}, v(\cdot, t_{n-1}+) \right)_{\Sigma \cup S} \right] = \int_{I_n} (s, v)_S \tag{10}$$

for all $v \in V_q$ and $n \in \mathbb{N}$, where $[w]_n = w(\cdot, t_n+) - w(\cdot, t_n-)$, $w_n^\pm = \lim_{s \to 0^\pm} w(t_n + s)$. Here

$$(u, v)_D = \int_D u \, v \,, \qquad u, v \in L^2(D)$$

denotes the standard scalar product of $L^2(D)$ for a domain $D \subset \mathbb{R}^3$. The source term $s \in L^2(L^2(S))$ is given by $\nabla \phi$ in equation (4).

In [11] it is shown, that the fully discrete scheme obtained by the DG(0)-Method converges to the solution of the continuous solution of a mixed elliptic-parabolic problem. Moreover, an explicit bound for the a priori error is presented. This estimate can also be established for the electromagnetic problem. We do not go into details here.

4 Coupling Strategies

The coupling between the mechanical and electromagnetic subsystems takes the form of the Lorentz force, the electromotive intensity, and the current geometry of the workpiece. The simulation of the coupled process is carried out on two meshes, one for the electromagnetic field computation and another for the mechanical structure. At a certain time step, the magnetic vector potential depending on the input amperage and the position of the structure is computed in the electromagnetic mesh and Lorentz force as well as electromotive intensity are derived. After that, these quantities are transferred into the mechanical mesh and imposed on the structure to determine its corresponding position. The altered position of the work piece is then transferred into the electromagnetic mesh and a corrected force distribution is computed. The two steps *field computation* and *structure simulation* are iterated until the electromagnetic fields and the position of the structure do not change in the scope of accuracy. This iterative scheme guarantees that the correct loads are computed for the mechanical structure, namely those connected to the new position of the work piece. When an equilibrium is attained, the next time step is started.

A natural discretization of the field equations leads to a moving mesh for the mechanical system, representing its current configuration and a fixed Eulerian mesh for the electromagnetic field. However, this approach implies serious difficulties concerning the data transfer between the two meshes: In those areas of the electromagnetic mesh currently covered by the moving structure a diffusive process with a positive finite diffusivity takes place, while outside this region the diffusivity is infinite such that the equilibrium state of the field is immediately assumed. Such a change alters the local discretization since a contribution to the mass matrix is present as soon as a point is covered by the structure and it disappears when it is uncovered again. It has turned out that this change of the discretization causes oscillations in the time derivative $\partial a/\partial t$ of the vector potential and, thus, in the Lorentz force. Newertheless, averaged quantities can sufficiently accurate be determined with this approach. In [10], it was successfully applied to compute the deformation of a mechanical structure even with relatively coarse discretizations. By the integration of Lorentz forces and due to the time stepping algorithm the above mentioned oscillations are smoothed out. However, as soon as a good and efficient approximation of the forces applied on the mechanical structure is required, an arbitrary Lagrangian Eulerian (ALE) formulation leads to much better results. In this approach, the electromagnetic mesh is adapted to the moving structure such that always the same elements are covered by the moving mechanical structure. Consequently, the character of the discretization in a particular element does never change, which avoids those jumps of a. In contrast to remeshing strategies, this approach preserves the combinatorial structure of the mesh, which allows an effective solution of the arising huge systems of linear equations. The discrete field equations on the electromagnetic mesh have to be reformulated such that the movement of the mesh is correctly considered. Surprisingly, the resulting field equations simplify. Instead of working with the partial time derivative $\partial a/\partial t$, it is convenient in this case to employ the material time derivative $\dot{a} = \partial a/\partial t + \nabla a \times v$ since its discretization is a function of the vertices of the moving mesh inside the mechanical structure rather than of spatial points. Thus, no interpolation is necessary to link past data to current data. Inside the fixed tool coil $\dot{a} = \partial a/\partial t$ applies and in

the air surrounding the tool coil and the workpiece the field assumes an equilibrium position instantaneously, which is explicitly neither depending on values of $\partial a/\partial t$ nor on values of a from a preceding time step. The weak semi-gauged form for the electromagnetic problem then takes the form

$$\int_\Omega \frac{1}{\mu} \operatorname{curl} a \operatorname{curl} a^* + \int_\Sigma \gamma_\Sigma a^* \dot{a} + \int_S \gamma_S a^* \dot{a} = -\int_S \gamma_S a^* \nabla\phi$$
$$\int_S \nabla\phi \nabla\phi^* = 0 \tag{11}$$

with constant conductivities γ_Σ for the work piece and γ_S for the tool coil.

5 Adaptivity

We employ two different concepts of adaptivity: The first concept is based on a precise physical understanding of the forming process at hand. Its advantage is the enormous gain in efficiency it leads to. Its drawback is that the more efficient it is the more restricted is its use to a particular forming situation. The second method is based on quantities that are dertermined from a numerical simulation. It is robust in the sense that it applies to a large class of problems without the need of any adaptations. Figure 1 shows a mesh that has automatically be adapted to the numerical requirements of a mixed elliptic-parabolic problem. The interface region between the parabolic area and the elliptic area is finely resolved [see 21].

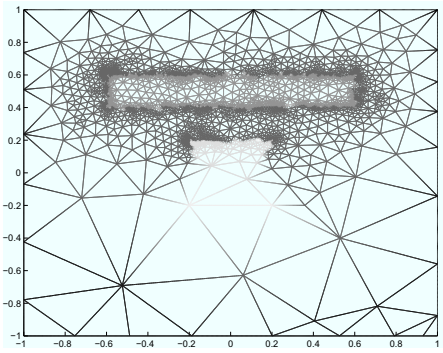

Figure 1: Automatically generated mesh adapted to the numerical requirements of a mixed elliptic parabolic problem

5.1 Adaptivity Based on a Physical Understanding of the Process

From a physical analysis of the process it is clear that after the first half wave of the triggering current has passed by, no more significant amount of energy is transmitted into the work piece. The forming process is then driven by predominantly inertial forces. To correctly meet the particular instance after which no significant energy transmission arises, criteria estimating the transmitted energy from data obtained during the simulation have been developed [1, 2]. Moreover, due to a retarded field expansion caused by magnetic diffusion, the area above the work piece is nearly free of a magnetic field. Hence we can a priori choose a very

coarse discretization there. In addition, a numerical scheme has been developed, that allows for different discretization levels for the electromagnetic and for the mechanical meshes in the context of an ALE-formulation. This is essential, when a shell formulation is coupled with th electromagnetic field computation as in [1, 2]. The influence of these modifications have thoroughly be studied [1, 2]. It has come out that the computational times could be reduced to approximately 1/10 of the original computational time.

5.2 Auto Adaptivity

Dual weighted residual error estimators represent an appropriate approach to error control for problems of the type described above. They allow a control of exactly those quantities which are of interest (see, e.g., [22]). Applied to a staggered solution algorithm, such techniques enable also to control the error of the quantities that realize the coupling between the two subsystems. Thus, error accumulation due to the coupling procedure can be reduced by mesh adaption in both subsystems. To construct a dual weighted residual error estimator for a simultaneous time- and space-adaptive scheme, we first introduce the notations

$$B(u,v) = \sum_{n=1}^{N} \int_{I_n} \left[(\dot{a}^h, v)_{\Sigma \cup S} + A(a^h, v) \right] + \sum_{n=1}^{N} ([a^h]_n \, , v(\cdot, t_{n-1}+))_{\Sigma \cup S}$$

for $u, v \in L^2(H_{\mathrm{curl}})$ and

$$L(v) = \int_I (s,v)_\Sigma$$

for $v \in L^2(H_{\mathrm{curl}})$. The forms B and L are bilinear on $L^2(H_{\mathrm{curl}})$. For the solution a^h of the discrete problem, we obtain

$$B(a^h, v) = L(v)\,, \qquad v \in V\,.$$

Since the solution of the originally problem is continuous with respect to the time variable t, all jump contributions $[a]_n$ cancel out, and we have the representation

$$B(a,v) = L(v)\,, \qquad v \in L^2(H_{\mathrm{curl}})\,.$$

The primal residual R^p is defined by

$$R^p(v) = B(e,v) = L(v) - B(a^h, v)\,, \qquad v \in L^2(H_{\mathrm{curl}}(\Omega))$$

with $e = a - a^h$. It possesses the explicit representation

$$R^p(v) = \int_I (s,v)_S - \sum_{n=1}^{N} \int_{I_n} \left[(\dot{a}^h, v)_{\Sigma \cup S} + A(a^h, v) \right] - \sum_{n=1}^{N} ([a^h]_{n-1} \, , v(\cdot, t_{n-1}+))_{\Sigma \cup S}\,. \qquad (12)$$

With the help of the primal residual we can represent the error in a quantity of interest, which we consider as given by a linear functional J on $L^2(H_{\mathrm{curl}}(\Omega))$. Due to linearity, we have

$$J(a) - J(a^h) = J(a - a^h) = J(e)\,.$$

By the Riesz representation theorem, there exists $\zeta \in L^2(H_{\mathrm{curl}}(\Omega))$ such that

$$B(v,\zeta) = J(v)\,, \qquad v \in L^2(H_{\mathrm{curl}}(\Omega))\,. \tag{13}$$

The field ζ is the solution of the so called dual problem. This is also a well defined evolution problem with similar analytic properties as the primal problems, but with inverted course of time. If, e.g., J is a functional that only depends on $a(\cdot, t_n)$, then J defines initial conditions for the dual problem. Now let ζ^h be an approximation to the solution ζ of the dual problem (13) computed via (10) based on the same mesh as was used to determine a^h. Galerkin-orthogonality yields

$$J(e) = B(a - a^h, \zeta) = B(e, \zeta - \zeta^h) = R^p(\zeta - \zeta^h)\,, \tag{14}$$

where ζ^h is an approximation to the dual solution ζ.

Considering (12), we notice that the error representation given in (14) does not depend on the continuous primal solution a, but only on a^h and on $\zeta - \zeta^h$. The first quantity is a posteriori known, i.e. after a finite element computation has been carried out. If mesh adaptation is the major issue, an approximation of $\zeta - \zeta^h$ is sufficiently accurately determined from ζ^h by a patch-recovery technique. To avoid purely technical discussions, we confine our considerations to finite element meshes that consist of tetrahedra elements and that possess no elements T that contain both inner points of Σ and of $\Omega \setminus \Sigma$ and no elements that contain both inner points of S and of $\Omega \setminus S$. The case of hexahedral elements is treated similarly. The following localized representation of the error can now be derived: With the above notations, we have for $q = 0$ and Nédélec elements of lowest order

$$\begin{aligned} J(e) = & \sum_{\substack{1\le n\le N \\ T\in\mathcal{T}, T\subset\overline{\Sigma\cup S}}} \left[\int_{I_n\times T} s\,(\zeta - \zeta^h) + \int_T [a^h]_{n-1} \left(\zeta - \zeta^h\right)(\cdot, t_{n-1}+) \right] \\ & + \sum_{\substack{1\le n\le N \\ F\in\mathcal{F}}} \int_{I_n\times F} (\zeta - \zeta^h)\, \lfloor \mathrm{curl}\, a^h \rfloor_F\, n_F\,. \end{aligned} \tag{15}$$

Here, $\mathcal{F}$ denotes the set of all faces of the triangulation and $\lfloor \mathrm{curl}\, a^h \rfloor_F$ is the vector consisting of the jumps of $\mathrm{curl}\, a^h$ when passing over the face F. Further, n_F denotes a unit normal vector of the face E pointing outwards. Note the representation given above can be applied both if a^h and ζ^h have been computed via a problem that has explicitly been gauged in the air region or via a non gauged numerical scheme as e.g. proposed by [13]. A full exploitation of the gain in efficiency that would follow when the above error estimator is applied for local mesh adaptation requires to allow for individual time steps in different spatial areas of the discretization. Hence time stepping would become completely implicit. However, having an efficient multi-grid solver at hand, the complexity of a fully implicit treatment would not be significantly larger than that of an explicit scheme for sufficiently high numbers of unknown. Hence we consider the use of the above described technique for time-space mesh-adaptivity as promising for the simulation of large problems of technological relevance. While hanging nodes in time have pointed out to be a major problem for time-space adaptive methods for hyperbolic problem, the situation for parabolic problems looks much better. Errors entering due to mesh irregularities are damped due to the energy dissipation typical of parabolic problems. The numerical implementation and validation of the here presented techniques for a posteriori error control represents work in progress.

6 Conclusions and Future Developments

Although a scientific base for a virtual design for electromagnetic forming processes has been founded, further research is required to establish methods that cope with the large number of unknowns that result from the discretization of typical three dimensional forming situations. Many strategies to reduce computational time have been mentioned in this article. In the sense of a robust algorithm that can be applied to many situations an auto adaptive scheme seems to be very promising. Such a scheme adapts the finite element mesh to the numerical requirements. Dual weighted residual error estimators allow for the control of a quantity of interest. Such a quantity usually results from practical consideration concerning the requirements a formed work piece should match.

References

[1] *Unger, J.*: Modeling and simulation of coupled electromagnetic field problems with application to model identification and metal forming. Ph.D. thesis, Universität Dortmund, 2007.

[2] *Unger, J.*; *Stiemer, M.*; *Svendsen, B.*; and *Blum, H.*: Strategies for 3D simulation of electromagnetic forming processes. Journal of Materials Processing Technology, volume 199: pp. 341–362, 2008.

[3] *Svendsen, B.* and *Chanda, T.*: Continuum thermodynamic modeling and simulation of electromagnetic forming. Technische Mechanik, volume 23: pp. 103–112, 2003.

[4] *Svendsen, B.* and *Chanda, T.*: Continuum thermodynamic formulation of models for electromagnetic thermoinlastic materials with application to electromagnetic metal forming. Cont. Mech. Thermodyn., volume 17: pp. 1–16, 2005.

[5] *Stiemer, M.*; *Unger, J.*; *Blum, H.*; and *Svendsen, B.*: Fully-coupled 3D simulation of electromagnetic forming. In *Proceedings of the 2nd International Conference on High Speed Forming*, pp. 63–72. ICHSF 2006, 2006.

[6] *Stiemer, M.*; *Unger, J.*; *Blum, H.*; and *Svendsen, B.*: An arbitrary Lagrangian Eulerian approach to the three dimensional simulation of electromagnetic forming. 2006. Submitted.

[7] *Reese, S.*; *Svendsen, B.*; *Stiemer, M.*; *Unger, J.*; *Schwarze, M.*; and *Blum, H.*: On a new finite element technology for electromagnetic metal forming processes. Archive of Applied Mechanics (Ingenieur Archiv), volume 74: pp. 834–845, 2005.

[8] *Reese, S.*: A large deformation solid-shell concept based on reduced integration with hourglass stabilization. International Journal for Numerical Methods in Engineering, volume 69: pp. 1671–1716, 2007.

[9] *Moon, F.*: Magnetic interactions in solids. Springer-Verlag, 1980.

[10] *Stiemer, M.*; *Unger, J.*; *Blum, H.*; and *Svendsen, B.*: Algorithmic formulation and numerical implementation of coupled multifield models for electromagnetic metal forming simulations. Int. J. Numer. Methods Engrg., volume 68: pp. 1301–1328, 2006.

[11] *Stiemer, M.*: Dicontinuous Galerkin methods for mixed parabolic-elliptic partial differential equations. 2006. Submitted.

[12] *Zaglmayr, S.*: High Order Finite Elements for Electromagnetic Field Computation. Johannes Kepler Universität, Linz (Dissertation), 2006.

[13] *Sterz, O.*: Modeling and numerical methods of time harmonic eddy currents in three dimensions. (Modellierung und Numerik zeitharmonischer Wirbelstromprobleme in 3D. Whitney-Elemente, adaptive Mehrgitterverfahren, Randelemente.). Heidelberg: Universität Heidelberg, Naturwissenschaftlich-Mathematische Gesamtfakultät (Dissertation 2003). xv, 185 p. , 2003.

[14] *Hiptmair, R.*: Multigrid method for Maxwell's equation. SIAM J. Numer. Anal., volume 36(1): pp. 204–225, 1986.

[15] *Nédélec, J. C.*: Mixed Finite Elements in $\mathbb{R}^3$. Numerische Mathematik, volume 35: pp. 315–341, 1980.

[16] *Nédélec, J. C.*: A New Family of Mixed Finite Elements in $\mathbb{R}^3$. Numerische Mathematik, volume 50: pp. 57–81, 1986.

[17] *Eriksson, K.* and *Johnson, C.*: Adaptive finite element methods for parabolic problems I: A linear model problem. SIAM J. Numer. Anal., volume 28(1): pp. 43–77, 1991.

[18] *Eriksson, K.* and *Johnson, C.*: Adaptive finite element methods for parabolic problems II: Optimal error estimates in $L_\infty L_2$ and $L_\infty L_\infty$. SIAM J. Numer. Anal., volume 32(3): pp. 706–740, 1995.

[19] *Eriksson, K.* and *Johnson, C.*: Adaptive finite element methods for parabolic problems IV: Nonlinear Problems. SIAM J. Numer. Anal., volume 32(6): pp. 1729–1749, 1995.

[20] *Eriksson, K.* and *Johnson, C.*: Adaptive finite element methods for parabolic problems V: Long-Time Integration. SIAM J. Numer. Anal., volume 32(6): pp. 43–77, 1995.

[21] *Stiemer, M.*: Error control for discretizations of electromagnetic-mechanical multifield problems. In *Proceedings of the ENUMATH conference 2005*, pp. 239–246. Santiago de Compostela, 2006.

[22] *Becker, R.* and *Rannacher, R.*: A feed-back approach to error control in finite element methods: Basic analysis and examples. EAST-WEST J. Numer. Math., volume 4: pp. 137–164, 1996.